

Trimer Formation and Metal-Insulator Transition in Orbital Degenerate Systems on a Triangular Lattice

Junki YOSHITAKE* and Yukitoshi MOTOME

Department of Applied Physics, University of Tokyo, 7-3-1 Hongo, Bunkyo, Tokyo 113-8656, Japan

As a prototypical self-organization in the system with orbital degeneracy, we theoretically investigate trimer formation on a triangular lattice, as observed in LiVO_2 . From the analysis of an effective spin-orbital coupled model in the strong correlation limit, we show that the previously-proposed orbital-ordered trimer state is not the lowest-energy state for a finite Hund's-rule coupling. Instead, exploring the ground state in a wide range of parameters for a multiorbital Hubbard model, we find an instability toward a different orbital-ordered trimer state in the intermediately correlated regime in the presence of trigonal crystal field. The trimer phase appears in the competing region among a paramagnetic metal, band insulator, and Mott insulator. The underlying mechanism is nesting instability of the Fermi surface by a synergetic effect of Coulomb interactions and trigonal-field splitting. The results are compared with experiments in triangular-lattice compounds, LiVX_2 ($X=\text{O}, \text{S}, \text{Se}$) and NaVO_2 .

KEYWORDS: cluster formation, trimer, multiorbital Hubbard model, triangular lattice, orbital order, metal-insulator transition

Orbital degree of freedom plays a decisive role in many transition metal compounds.^{1–3}) Orbital ordering and its fluctuation affect magnetic, transport, and structural properties in a complicated manner through the coupling to spin, charge, and lattice degrees of freedom. One of the characteristic phenomena, particularly observed in geometrically-frustrated systems, is spontaneous formation of clusters. It is a structural phase transition to form ‘molecules’ of transition metal atoms by periodic modulation of the lattice structure. For example, CuIr_2S_4 shows a formation of octumers⁴) and AlV_2O_4 shows heptamers⁵) on their pyrochlore networks of Ir or V, and the importance of d -electron orbitals was theoretically pointed out.^{6,7}) The spontaneous formation of ‘molecules’ has attracted increasing interest as emergent physics in the systems with multiple degrees of freedom.

A prototypical example of such clusters is a trimer in a quasi-two-dimensional compound LiVO_2 .^{8,9}) In this system, each V^{3+} cation has two $3d$ electrons in threefold t_{2g} orbitals on average, and forms triangular lattices. The compound exhibits a first-order structural phase transition at $T_c \simeq 500$ K, accompanied by a sudden drop of the magnetic susceptibility.^{8,12,14}) Below T_c , V-V bonds are periodically modulated in each layer to form V_3 trimers.^{9–12}) The trimer formation was first interpreted by a charge-density-wave instability associated with the V clustering.^{9,13}) A spin-Peierls type scenario was also considered to account for the spin-singlet nature below T_c .¹⁴) Later, Pen *et al.* pointed out a crucial role of orbital ordering.¹⁵) It was claimed that LiVO_2 is a Mott insulator and the trimers are stabilized as the $S = 1$ spin-singlet objects under a particular ordering of the t_{2g} orbitals.

Experimentally, however, it is not clear to what extent the electron correlation plays an important role in LiVO_2 . The spin gap in the low-temperature(T) trimer phase was estimated to be $\Delta_s \sim 1600$ K,¹⁴) which is com-

parable to the charge gap estimated from T dependence of the resistivity, $\Delta_c \sim 0.14$ eV.¹²) In addition, the Curie-Weiss temperature estimated from the magnetic susceptibility for $T > T_c$ is ~ -1500 K,¹²) whose magnitude is also comparable to Δ_c . These facts clearly contradict with the local moment picture under the strong correlation. Recently, it was also shown that the substitution of O by S or Se makes the system metallic.¹⁷) This suggests that LiVO_2 is located in the vicinity of correlation-driven metal-insulator transition. It is highly nontrivial how the itinerant tendency is compatible with the $S = 1$ local moment formation expected for the strong electron correlation. Hence, the origin of the trimer formation in LiVO_2 is still in dispute. It is desired to revisit the problem theoretically for clarifying the role of electron correlation and orbital degree of freedom.

In this Letter, we address this issue by carefully examining various orbital and spin orderings in a wide range of electron correlation. In particular, revisiting the strong correlation picture, we show that the system is likely to exhibit a four-sublattice spin and orbital ordering in the ground state, not the previously-proposed trimer state. We, however, identify a different orbital-ordered trimer state in the intermediately correlated region on the verge of metal-insulator transition, where the Coulomb interactions work cooperatively with the trigonal-field splitting. The results provide underlying mechanism in the self-organization in orbital degenerate systems close to metal-insulator transition.

We start with a multiorbital Hubbard model for the threefold t_{2g} orbitals. The Hamiltonian is given as

$$\mathcal{H} = - \sum_{\langle ij \rangle} \sum_{\alpha\beta} \sum_{\tau} t_{ij}^{\alpha\beta} \left(c_{i\alpha\tau}^\dagger c_{j\beta\tau} + \text{H.c.} \right) + \frac{1}{2} \sum_i \sum_{\alpha\beta\alpha'\beta'} \sum_{\tau\tau'} U_{\alpha\beta\alpha'\beta'} c_{i\alpha\tau}^\dagger c_{i\beta\tau'}^\dagger c_{i\beta'\tau'} c_{i\alpha'\tau}, \quad (1)$$

where the first term is the electron hopping between the

*E-mail address: yoshitake@aion.t.u-tokyo.ac.jp

nearest-neighbor sites $\langle ij \rangle$ on a triangular lattice; α, β denote the three t_{2g} orbitals, d_{xy} , d_{yz} , or d_{zx} ; τ, τ' denote the spins, \uparrow or \downarrow . The second term represents the on-site Coulomb interactions, for which we use the standard parametrizations, $U_{\alpha\beta\alpha'\beta'} = U'\delta_{\alpha\alpha'}\delta_{\beta\beta'} + J_H(\delta_{\alpha\beta'}\delta_{\beta\alpha'} + \delta_{\alpha\beta}\delta_{\alpha'\beta'})$ and $U = U' + 2J_H$. Following the previous study,¹⁵⁾ we here consider the overlap integrals of σ -bond orbitals only and take them as the energy unit, $t_\sigma = 1$. We fix the electron density at $n = \sum_{i\alpha} \langle n_{i\alpha} \rangle / N = 2$, i.e., two electrons per site on average (N is the number of sites).

First, we consider the strong correlation limit of the model in Eq. (1). The second order perturbation in t_σ/U gives an effective spin-orbital Hamiltonian¹⁾ in the form

$$\mathcal{H}_{\text{eff}} = -J \sum_{\langle ij \rangle} [h_{\text{o-AF}}^{(ij)} + h_{\text{o-F}}^{(ij)}], \quad (2)$$

where $h_{\text{o-AF}}^{(ij)} = (A + B\vec{S}_i \cdot \vec{S}_j)(n_{i\alpha(ij)}\bar{n}_{j\alpha(ij)} + \bar{n}_{i\alpha(ij)}n_{j\alpha(ij)})$ and $h_{\text{o-F}}^{(ij)} = C(1 - \vec{S}_i \cdot \vec{S}_j)n_{i\alpha(ij)}n_{j\alpha(ij)}$. Here \vec{S}_i is the $S = 1$ spin operator at site i , $\alpha(ij)$ is the orbital which has the σ -bond overlap between the sites i and j , and $\bar{n}_{i\alpha(ij)} = 1 - n_{i\alpha(ij)}$. The coefficients are given as $J = t_\sigma^2/U$, $A = (1 - \eta)/(1 - 3\eta)$, $B = \eta/(1 - 3\eta)$, $C = (1 + \eta)/(1 + 2\eta)$, and $\eta = J_H/U$. The same effective model was studied for LiVO_2 .¹⁵⁾ It was shown that an $S = 1$ spin-singlet state with trimer-type orbital ordering [Fig. 1(a)] has the same ground-state energy as an antiferromagnetic (AF) state with a ‘square-type’ orbital ordering [Fig. 1(b)] in the limit of $\eta = 0$, i.e., $U = U'$ and $J_H = 0$. However, it was not clarified how a finite Hund’s-rule coupling modifies the results, and moreover, whether there are other competing states.

In order to search the ground state of the model in Eq. (2) in an unbiased way, we performed Monte Carlo (MC) simulation at low T for the classical counterpart of the model, namely, by replacing the $S = 1$ operators by the classical vectors with unit length. The results indicate that, for $\eta > 0$, a four-sublattice ferrimagnetic state shown in Fig. 1(c) is selected as the lowest-energy state as $T \rightarrow 0$.

On the basis of the MC result, we compare the ground-state energy of the ferrimagnetic state with other several typical states, as plotted in Fig. 2. Here we consider four states in Figs. 1(a)-(d). For the states (b)-(d), the ground-state energies are analytically obtained as $E_{\text{sq-AF}} = -4CJ$, $E_{\text{ferri}} = -(2A + B + 2C)J$, $E_{120\text{-AF}} = -(2A - B + 3C/2)J$, respectively, by treating the model (2) at the classical level. For the trimer state (a), assuming the $S = 1$ spin-singlet state in each trimer, namely, $\langle \vec{S}_i \cdot \vec{S}_j \rangle = -1$ for the intra-trimer bonds, and neglecting the inter-trimer spin correlations, we obtain $E_{\text{trimer}} = -(2A + 2C)J$. The comparison indicates that the four-sublattice ferrimagnetic state gives the lowest energy for $\eta > 0$, consistent with the MC search. The energy is even lower than the previously-proposed trimer state.¹⁸⁾ E_{ferri} will be lowered when considering quantum fluctuations beyond the classical level, such as the spin wave contribution. Therefore, our results strongly suggest that the trimer state proposed in Ref.¹⁵⁾ is not the

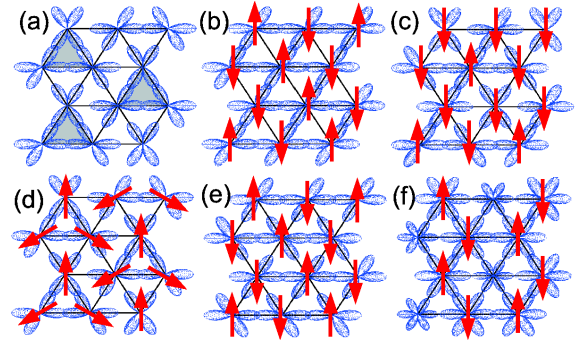


Fig. 1. (Color online). Schematic pictures of the spin-orbital ordered states: (a) orbital trimer state proposed in Ref. 15, (b) AF state with square-type orbital ordering, (c) ferrimagnetic state with four-sublattice spin-orbital ordering, (d)-(f) Hartree-Fock solutions appearing in the phase diagram in Fig. 3(a). Only dominant orbitals are drawn by lobes in each figure. Arrows represent spins. In (a), the shaded triangles denote the trimers with spin-singlet formation.

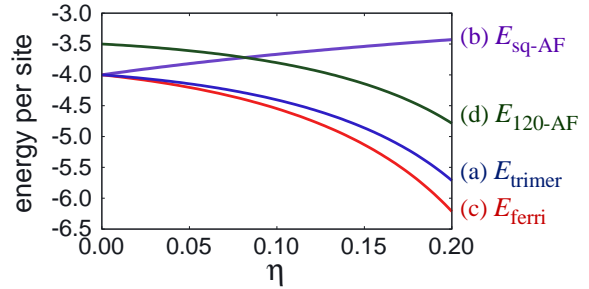


Fig. 2. (Color online). Ground-state energy of the model (2) for the four states in Figs. 1(a)-(d) as a function of $\eta = J_H/U$. See text for details.

ground state in the strong correlation limit, and is likely taken over by the four-sublattice ferrimagnetic state in Fig. 1(c).

The above considerations in the large- U limit lead us to go back to the multiorbital Hubbard model given by Eq. (1) and explore another possibility for the trimer formation. In the following analysis, we extend the model by including the trigonal distortion of VO_6 octahedra which is inherent in the layered materials. That is, we consider an additional term to Eq. (1) given by

$$\mathcal{H}_D = \frac{D}{2} \sum_i \sum_{\alpha \neq \beta} \sum_{\tau} c_{i\alpha\tau}^\dagger c_{i\beta\tau}, \quad (3)$$

which splits the t_{2g} levels into a_{1g} singlet and e'_g doublet by $3D/2$. The sign and magnitude of D is strongly dependent on the detailed band structure including the t_{2g} - e_g hybridization.¹⁹⁾ In the following calculations, we consider the case of $D > 0$ which lowers the a_{1g} level.²⁰⁾

To map out the ground-state phase diagram in a wide parameter region, we employ the Hartree-Fock approximation. In the calculations, we take the 12-site unit cell in the form shown in Fig. 1, and consider 24×24 array of the unit cell with appropriate boundary conditions. This enables to incorporate both three- and four-sublattice orders, such as the trimer and ferrimagnetic states.

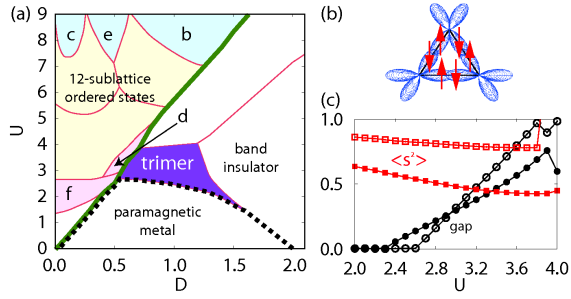


Fig. 3. (Color online). (a) Ground-state phase diagram for the multiorbital Hubbard model at the electron density $n = 2$ obtained by the Hartree-Fock calculation. The thick curve represents the boundary between magnetic and nonmagnetic solutions (the upper left is magnetic). The dotted curve represents the metal-insulator transition line. Spin and orbital patterns for the states b-f are drawn in Figs. 1(b)-(f), respectively. (b) A schematic picture of the spin and orbital state in the trimer phase. (c) Total spin $\langle S^2 \rangle$ (square) and energy gap (circle) as a function of U at $D = 0.7$ (open) and 1.1 (closed).

Figure 3(a) shows the representative result for the ground-state phase diagram as functions of U and D . We take $\eta = 0.1$, i.e., $U' = 0.8U$ and $J_H = 0.1U$. When $U = 0$, the system exhibits a metal-insulator transition from paramagnetic metal to band insulator at $D = 2$ by the trigonal-field splitting of a_{1g} and e'_g bands. On the other hand, at $D = 0$, the system is insulating for all $U > 0$ because of the perfect nesting of the Fermi surface. In the large- U region, we obtain the four-sublattice orbital-ordered ferrimagnetic state [Fig. 1(c)], in agreement with the above result for the large- U effective model in Eq. (2). We, however, do not find any trimer-type threefold ordering in the entire range of U at $D = 0$.

When D and U become both finite, the system exhibits a variety of phases with different spin and orbital ordering.²¹⁾ Among them, the most interesting phase is the three-sublattice spin-orbital ordered state in the range of $0.5 \lesssim D \lesssim 1.5$ and $2 \lesssim U \lesssim 4$. This phase is insulating [gap is plotted in Fig. 3(c)] and nonmagnetic, appearing on the verge of the metal-insulator boundary and the magnetic-nonmagnetic boundary [dotted and thick curves in Fig. 3(a), respectively]. In other words, it is stabilized in the competing region among the paramagnetic metal, band insulator, and magnetic Mott insulator.

The three-sublattice ordered state shows a trimer-type orbital ordering, similar to that in the previously-proposed trimer state in Ref. 15. The spin state is, however, quite different from the $S = 1$ spin-singlet; each of the two σ -bond orbitals is dominantly occupied by up or down electron at each site, and the intersite σ bond is formed by a pair of the spin-up and down orbitals, as shown in Fig. 3(b). This is different from the $S = 1$ high-spin state with the total spin $\langle S^2 \rangle \simeq 2$ [see Fig. 3(c)].

This state is distinct from that expected in the two well-known limits for the bond formation. One is a spin-Peierls type instability in the strong coupling picture, as discussed in Refs. 14 and 15; in this case, the spin-singlet bond is formed through the superexchange coupling between the localized $S = 1$ spins. The other limit is the

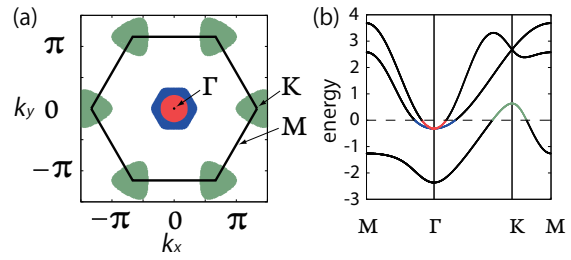


Fig. 4. (Color online). (a) Fermi surfaces at $(D, U) = (1, 2)$ obtained by the Hartree-Fock calculation. The large hexagon represents the first Brillouin zone. Dark grey circle and hexagon around the Γ point represent electron pockets. The light grey triangles around the K points represent hole pockets. (b) Corresponding band dispersions. Fermi energy is set to be zero.

Peierls instability to form a bonding orbital in the weak coupling picture;¹⁶⁾ here each bonding orbital is unpolarized and spins do not play an important role. In our trimer state, the bonding orbitals are spin polarized to form the intersite spin-up and down pairs, whereas the polarization is cancelled at each site between two occupied orbitals. This is considered to be a compromise between the spin-Peierls-type superexchange physics and the Peierls-type bonding orbital formation.

The stabilization mechanism of the trimer-type orbital ordering is understood as follows. In the paramagnetic metal close to the metal-insulator phase boundary, one of the three bands makes a hole pocket of the Fermi surface around the K point, and the other two form two electron pockets around the Γ point, as exemplified in Fig. 4 for the case of $(D, U) = (1, 2)$. As approaching the metal-insulator phase boundary, the pockets shrink and the nesting is developed between the hole pocket and electron pockets. At some point under sufficient nesting, finite Coulomb interactions induce an instability toward some symmetry breaking, as often seen in spin- or charge-density-wave transitions. In the present case, the nesting is between the different orbitals, and therefore, such instability gives rise to an orbital ordering. The ordering is of period three because the vector connecting the Γ and K points is one third of the reciprocal lattice vector. Because this picture is simple and robust in the presence of the trigonal-field splitting, we believe that the nesting mechanism and the resulting trimer-type orbital order will survive even when going beyond the mean-field approximation and including fluctuation effects.

Let us discuss our results in comparison with experiments. First of all, our nonmagnetic trimer state appears in the intermediately correlated region, which is in qualitative agreement with experiments in LiVO_2 . In particular, the fact that our trimer is in between the band insulator and Mott insulator well accounts for the comparable energy scale between the spin and charge gap. The calculated values of the gap, shown in Fig. 3(c), is on the order of 0.1 eV, when considering the bandwidth ~ 4 eV in the first-principles calculation.²⁰⁾ This is compared favorably with the experimental estimate.¹²⁾ Furthermore, our trimer state is on the border of the metal-insulator transition to the paramagnetic metal; this agrees with the

experimental trend in the substituted materials LiVX_2 ($X=\text{O}, \text{S}, \text{Se}$).¹⁷⁾ Our trimer state is nonmagnetic, but each occupied orbital is spin polarized under the electron correlation, which is clearly distinct from the low-spin nonmagnetic band insulator under strong trigonal field: It is desired to reexamine the x-ray absorption spectra, which was argued to be consistent with the high-spin state,²²⁾ by taking our spin-orbital ordered trimer state into consideration. To confirm our scenario, it is important to identify the band structure and the Fermi surfaces in the metallic compounds, such as LiVSe_2 , experimentally or by first-principles calculations. A quantitative estimate of Coulomb interactions is also helpful. It will be also interesting to experimentally examine the effect of uniaxial pressure which dominantly affects D .

Interestingly, our phase diagram includes the square-type AF state [Fig. 1(b)] in the region $U \gtrsim 7$ for nonzero D . The spin-orbital order coincides with that in the lowest-temperature phase in a related compound NaVO_2 .²³⁾ The compound is indeed more strongly-correlated than LiVO_2 , evidenced by the larger charge gap and lattice constant. We, however, note that a LSDA+ U calculation predicted the opposite sign of D for NaVO_2 .²⁴⁾ Extension of our analysis in a wide range of parameters including $D < 0$ is left for future study.

In our study, we considered the σ -bond overlap t_σ only. We confirmed that our trimer state remains robust for more general band structure when t_σ is dominant. We note that the value of D for our trimer state is larger than that obtained by the first-principles calculation.²⁰⁾ We also note that U might be small compared to the estimate from fitting of the photoemission spectra for a related perovskite.²⁵⁾ The parameter range for our trimer state, however, may be extended to smaller D and larger U region when we include the concomitant lattice distortions with trimer formation, as observed in experiments. We confirmed this tendency by considering the model (1) on an isolated three-site cluster. Meanwhile, the cluster calculation predicts that another magnetic trimer state (d) is also extended and reach $D = 0$. We speculate that this state is related with the spin-singlet trimer state obtained in the exact diagonalization for a three-site cluster at $D = 0$ in Ref. 15. An interesting question is, in the presence of lattice modulation, how the magnetic and nonmagnetic trimer states are modified in more sophisticated calculations beyond the mean-field approximation. This problem is left for future study.

In conclusion, we have investigated the origin of the trimer formation in the Hubbard model with t_{2g} orbital degeneracy on a triangular lattice. We found that a nonmagnetic trimer state with three-sublattice spin-orbital ordering is stabilized by nesting between different orbitals on the border of metal-insulator transition under the trigonal crystal field. This state takes the most efficient of both the spin-Peierls instability assisted by orbital ordering in the strong coupling picture and the Peierls instability by forming bonding orbitals in the weak coupling picture. Our result underlies a general mechanism of the cluster formation in the intermediately-correlated orbital degenerate systems. It

also potentially provides comprehensive understanding of a variety of the ground states in the related compounds LiVX_2 ($X=\text{O}, \text{S}, \text{Se}$) and NaVO_2 .

Acknowledgment The authors thank D. Khomskii, H. Takagi, J. Matsuno, and N. Katayama for fruitful discussions. This research was supported by KAKENHI (No. 19052008, 17740244, and 16GS0129), and Global COE Program “the Physical Sciences Frontier.” Y. M. acknowledges the hospitality of KITP Santa Barbara, where a part of this work was done.

- 1) K. I. Kugel and D. I. Khomskii: Sov. Phys. Usp. **25** (1982) 231.
- 2) Y. Tokura and N. Nagaosa: Science **288** (2000) 462.
- 3) D. I. Khomskii: Phys. Scrip. **72** (2006) CC8.
- 4) P. G. Radaelli, Y. Horibe, M. J. Gutmann, H. Ishibashi, C. H. Chen, R. M. Ibberson, Y. Koyama, Y.-S. Hor, V. Kiryukhin and S.-W. Cheong: Nature (London) **416** (2002) 155.
- 5) Y. Horibe, M. Shingu, K. Kurushima, H. Ishibashi, N. Ikeda, K. Kato, Y. Motome, N. Furukawa, S. Mori and T. Katsufuji: Phys. Rev. Lett. **96** (2006) 086406.
- 6) D. I. Khomskii and T. Mizokawa: Phys. Rev. Lett. **94** (2005) 156402.
- 7) K. Matsuda, N. Furukawa, and Y. Motome: J. Phys. Soc. Jpn. **75** (2006) 124716.
- 8) P. F. Bongers: Dr. Thesis, University of Leiden, (1957).
- 9) J. B. Goodenough: *Magnetism and the Chemical Bond* (John Wiley and Sons, New York-London, 1963)
- 10) L. P. Cardoso and D. E. Cox: J. Solid State Chem. **72** (1988) 234.
- 11) K. Imai, H. Sawa, M. Koike, M. Hasegawa and H. Takei: J. Solid State Chem. **114** (1995) 184.
- 12) W. Tian, M. F. Chisholm, P. G. Khalifah, R. Jin, B. C. Sales, S. E. Nagler and D. Mandrus: Mater. Res. Bull. **39** (2004) 1319.
- 13) J. B. Goodenough, G. Dutta, and A. Manthiram: Phys. Rev. B **43** (1991) 10170.
- 14) M. Onoda, T. Naka and H. Nagasawa: J. Phys. Soc. Jpn. **60** (1991) 2550.
- 15) H. F. Pen, J. van den Brink, D. I. Khomskii and G. A. Sawatzky: Phys. Rev. Lett. **78** (1997) 1323.
- 16) R. E. Peierls: *Quantum Theory of Solids* (Oxford Univ. Press, Oxford, England, 1955), p. 108.
- 17) N. Katayama, M. Uchida, D. Hashizume, S. Niitaka, J. Matsuno, D. Matsumura, Y. Nishihata, J. Mizuki, N. Takeshita, A. Gauzzi, M. Nohara and H. Takagi: Phys. Rev. Lett. **103** (2009) 146405.
- 18) We can estimate the lower bound of E_{trimer} by decomposing the effective spin Hamiltonian into six-site clusters. The estimate is still higher than E_{ferri} .
- 19) S. Landron and M.-B. Lepetit: Phys. Rev. B **77** (2008) 125106.
- 20) S. Y. Ezhov, V. I. Anisimov, H. F. Pen, D. I. Khomskii and G. A. Sawatzky: Europhys. Lett. **44** (1998) 491.
- 21) The appearance of 12-site orders implies that larger unit cell is necessary to discuss the correct ordering patterns in this intermediate- U region. Other phases in the smaller U region are basically understood from the nesting of the Fermi surface. The phase extending near $U \sim 4D$ for $U \gtrsim 4$ exhibits a four-sublattice spin-orbital order; there, each orbital has spin polarization, but the polarization is cancelled at each site.
- 22) H. F. Pen, L. H. Tjeng, E. Pellegrin, F. M. F. de Groot and G. A. Sawatzky: Phys. Rev. B **55** (1997) 15500.
- 23) T. M. McQueen, P. W. Stephens, Q. Huang, T. Klimczuk, F. Ronning and R. J. Cava: Phys. Rev. Lett. **101** (2008) 166402.
- 24) T. Jia, Guoren Zhang and Zhi Zeng: Phys. Rev. B **80** (2009) 045103.
- 25) A. E. Bocquet, T. Mizokawa, K. Morikawa and A. Fujimori: Phys. Rev. B **53** (1996) 1161.